Adsorption of (*S*)-Histidine on Cu(110) and Oxygen-Covered Cu(110), a Combined Fourier Transform Reflection Absorption Infrared Spectroscopy and Force Field Calculation Study

E. Mateo Marti, Ch. Methivier, P. Dubot, and C. M. Pradier*

Laboratoire de Physico-Chimie des Surfaces, CNRS (UMR 7045)—Ecole Nationale Supérieure de Chimie de Paris, 11 rue Pierre et Marie Curie, 75005 Paris, France

Received: May 16, 2003; In Final Form: July 15, 2003

Adsorption of (*S*)-histidine on Cu(110), and Cu(110) modified by adsorbed oxygen, has been studied by reflection absorption infrared spectroscopy (RAIRS). The molecular form and the orientation of the histidine molecule were deduced from experimental RAIRS data; moreover, vibrational spectra were simulated with a molecular mechanics force field (MMFF) calculation to address vibrational modes and the geometry of the adsorbate. The molecule preferentially binds to the surface in its $HHis^-$ molecular form. On the metallic Cu(110) surface, the adsorption occurs via the carboxylate group (COO^-), with the two oxygen atoms equidistant from the surface, and via the dehydrogenated nitrogen of the imidazole group; the latter adopts an upright position with respect to the copper surface. The amino group (NH_2) is likely to be maintained close to the surface, thus facilitating the interaction with the metal. Preadsorption of oxygen ($\theta \approx 0.3$) on the copper surface induces minor changes in the molecular orientation: the ring tends to be less upright than in the absence of oxygen; the ring now interacts via its NH group as deduced from RAIRS and MMFF calculations. The molecule does not reorient with increasing oxygen coverage ($\theta \approx 0.6$), and no surface blocking was observed upon oxygen adsorption; both the orientation and the amount of histidine only slightly vary when the oxygen coverage is increased.

1. Introduction

The adsorption of large biological molecules such as proteins onto solid surfaces is of interest for many scientific and technological areas.[1,2] The creation of a controlled, well-ordered, and functional protein layer at a metal surface has become a challenging research field for biocatalysis, biosensors, biocompatibility of artificial implants in living systems, membrane technologies, and biocorrosion, among others. By creating well-defined immobilized systems, i.e., by controlling the metal−protein chemical interaction as well as the molecular orientation, the control of specific chemical and biological responses, such as antibody−antigen affinity or cell migration, can be expected.[3,4]

The chemical binding of proteins on metals can be modeled by studying the interactions of individual amino acids with surfaces. Because of their relatively simple structure in comparison with polypeptides and proteins, and since they are building blocks in the latter, amino acids can bring basic information about adsorption of proteins on a metal surface. The study of the simple amino acid can indeed assist in the understanding of more complex systems, where the conformation in the adsorbed state results in all of the individual interactions between amino acids and the surface, and among the amino acids. Only a few amino acid−metal systems have been, to our knowledge, extensively studied with a range of surface science techniques: glycine, alanine, and proline on Cu(110).[5−7]

We focus our study on (*S*)-histidine; there are 17 of these fragments in a bovine serum albumin (BSA) molecule, a protein that has often been used to investigate the role of a protein film upon bacterial adhesion or to test the specific properties of biosensors for instance.[8−10] Histidine likely plays an important role in the interaction process of BSA with solid surfaces as suggested by several authors.[11] This amino acid is also known to be involved in various biological processes related to enzyme action; it has medical applications as an antiinflammatory, a tissue growth and repair agent, and a helpful agent in rheumatoid arthritis.[12]

(*S*)-Histidine is a potential tridentate ligand having three coordinating sites, amino and imidazole nitrogen atoms and a carboxyl group. Its structures, these groups being protonated or not, are presented in Figure 1. This molecule possesses an imidazole ring in its side chain, which is a very important ligand for copper(II) in many biological systems;[13,14] imidazole is also known to be a versatile molecule in enzyme catalysis, at physiological pH values 7−8, and it is ionized, thus playing a major role in the buffer action of proteins.[15] The imidazole ring can indeed readily switch between different states, protonated or not, and catalyze the formation or the breaking of chemical bonds. It is also important to mention that imidazole-containing compounds are often used as corrosion inhibitors and as adhesion promoters particularly on copper;[16,17] this is an attractive feature especially in the printed circuit board industry.

Coming back to (*S*)-histidine, as one of the strongest metal coordinators among the amino acids, it participates in the binding of metal ions by proteins[18] as in the case of copper proteins, including superoxide dismutase and ascorbate oxidase proteins.[19] It has also been involved in the in vivo transport of copper between albumin and cells. The structures of metal−histidine complexes as a function of solution pD (D_2O solutions, modified by either DCl or NaOD, were used) have been inferred from infrared data, making clear the presence of monodentate, bidentate, and tridentate histidine complexes depending on the

* To whom correspondence should be addressed. E-mail: claire-marie-pradier@enscp.jussieu.fr.

10.1021/jp035355u CCC: $25.00
Published on Web 09/10/2003

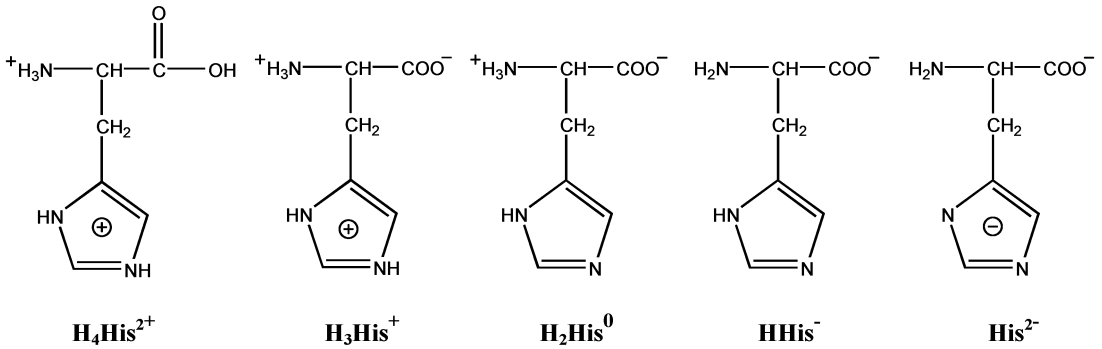

Figure 1. Structures of the ionic forms of histidine.

solution acidity.[18] X-ray studies in the solid state have demonstrated[20] that histidine can use each of the three potential coordination sites to bind metal ions.

However, the copper−histidine system is also a matter of controversy. Histidine−copper complexes have been studied[21] by potentiometry, calorimetry, and vibrational spectroscopy, yielding conclusions which are often contradictory. There are, in particular, conflicting views on the mode of histidine binding to copper(II). The system is complex[22] probably because, although metal atoms can coordinate to the three different binding sites of the molecule, copper tends to adopt square planar or grossly distorted octahedral[23] configurations as in cupric complexes, thus allowing only two sites in the histidine molecule to be bound simultaneously.[24] This makes clear the ambidentate nature of histidine.[23] Preference for one or the other binding sites, attached to the metal ion, will be governed by their ionic-state pH dependency. Let us add that (*S*)-histidine is a chiral molecule; this stresses the importance of controlling its binding mode. This literature survey shows how complex the histidine−metal interaction is; it underlines the need for a better knowledge of the binding mode of that molecule with copper. In that context, our novel approach, combining in situ infrared characterization of histidine, adsorbed on a well-defined copper surface, with a molecular mechanics force field (MMFF) code, to estimate the molecular conformation in the adsorbed state, is really promising.

We herein report reflection absorption infrared spectroscopy (RAIRS) data on the adsorption of the chiral amino acid (*S*)-histidine on a well-defined Cu(110) single-crystal surface. The adsorption of (*S*)-histidine was also studied on Cu(110) modified by preadsorption of oxygen for probing the influence of oxygen upon the interaction process with the surface. Auger electron spectroscopy (AES) and low-energy electron diffraction (LEED) were systematically operated before and after histidine dosing to check the copper surface chemical composition and structure. The combination of these three analytical surface science techniques gives us complementary information: (i) the nature and orientation of the adsorbed amino acid with respect to the surface during dosing and (ii) the nature of the chemical elements in the adsorbed layer, as well as the variations in their coverage on the surface after gas evacuation. The potential influence of the surface oxidation, or oxygen contamination, upon the adsorbed histidine form helps to clarify the links between structure and reactivity of amino acids on more "real" solid surfaces.

The spectrum of pure histidine, and pure imidazole, in its powder state, was also recorded by ATR (attenuated total reflection)-IR spectroscopy, i.e., with no restriction due to surface selection rules for a better identification of the vibrational groups.

To help us in the interpretation of the infrared spectra and find some information on the adsorbed molecular geometry, we used a molecular force field calculation to estimate the different vibrational frequencies and the orientation of $HHis^-$ adsorbed on the solid surface. This form was chosen because, as will be seen later, it is the most abundant in the adsorbed phase. Force field potentials were taken from MM2 and CHARMM parameters sets,[25,26] and the TINKER module was used for Hessian calculation and vibrational analysis.[27] RAIRS spectra were simulated by using surface selection rules where only vibrational modes with a nonzero dynamic dipole resultant perpendicular to the surface are active. In a first step, the molecular conformation for the adsorbed species was determined by force field energy minimization. Then, variations in the orientation of the cycle were simulated to determine which one was in best agreement with experimental RAIRS spectra.

2. Experimental Section

RAIRS spectra were recorded using a Nicolet magna 550 FT-IR spectrometer equipped with a liquid-nitrogen-cooled MCT wide-band detector with a spectral range of 650−4000 cm^{-1}. The spectrometer was interfaced to an ultra-high-vacuum (UHV) chamber with ZnSe windows. The Cu(110) single crystal was mounted in a multitechnique (UHV) chamber, with RAIRS, LEED, and AES facilities, and a base pressure of 1×10^{-9} mbar. The Cu(110) crystal was cleaned by cycles of Ar^+ ion sputtering, flashing, and annealing to ∼900 K. The annealing procedure ensured desorption of residual impurities and restored the crystallinity of the topmost atomic layers. The surface structure and cleanliness were monitored by LEED and AES before and after adsorption experiments.

(*S*)-Histidine (>99%) was obtained from the Sigma Chemical Co. and used without further purification. It was contained in a small electrically heated glass tube, separated from the main vacuum chamber by a gate valve, and differentially pumped by a turbomolecular pump. Before sublimation the (*S*)-histidine powder was outgassed at 355 K, then heated to 370 K, and dosed into the chamber. The dosing pressure was maintained around 2×10^{-8} mbar during the RAIRS measurements.

The RAIRS spectra were recorded in situ, throughout a continuous dosing regime, and ratioed against a reference background single-beam spectrum recorded on the clean Cu(110) crystal. All spectra were obtained at 8 cm^{-1} resolution, by co-addition of 256 scans.

(*S*)-Histidine adsorption was then investigated on oxygen-modified surfaces, at two different coverage values: oxygen was preadsorbed for 5 min at $P_{O_2} = 1 \times 10^{-6}$ mbar, leading to a p(2×1) LEED structure ($0.2 \leq \theta \leq 0.3$), or 10 min at $P_{O_2} =$

TABLE 1: Infrared Assignment for (*S*)-Histidine at Different pD Values (from ref 15) in Comparison with (*S*)-Histidine on Cu(110) at 300 K[a]

	(*S*)-histidine in D_2O						
assignment from the lit.	H_4His^{2+} (pD 0)	H_3His^{+} (pD 4.8)	H_2His^{0} (pD 8.1)	$HHis^{-}$ (pD 12.2)	His^{2-} (pD 14)	(*S*)-histidine/ Cu(110)	assignment from our spectra
C═O str	1737						
COO^- as str		1625	1619			1628	COO^- as str
				1579	1579	1575	NH_2 sciss
ring str	1603		1482	1483	1456	1469	
CH_2 bend	1444	1443	1441	1442	1443	1434	CH_2 bend
COO^- s str	1411	1406	1408	1413	1418	1412/1395	COO^- s str
CH_2 wag	1357	1354	1351				
		1333	1334	1327	1334		
CH bend/ring str	1321	1324	1317	1314		1310	CH bend/ring str
C−O str	1274						
CCN str	1108	1108	1109	1103	1104		
CH bend	1088		1097	1097	1082		
CH_2 rock	1022	1019	1020			1015	CH_2 rock
ring breathing			1005	1012	1010	980	ring breathing
ring mode			943	945	952		
CCN str/CC str	874	862				860	CCN str/CC str
ring mode			847	837	842	836	ring mode

[a] Key: str, stretch; as str, asymmetric stretch; s str, symmetric stretch; sciss, scissors

6×10^{-4} mbar after the crystal was heated to 900 K, leading to a c(6×2) LEED structure ($\theta \approx 0.67$).[28]

3. Results and Discussion

3.1. The Different Forms of Histidine. Before our RAIRS data are presented and discussed, it is helpful to describe the possible forms of the histidine molecule. Histidine, like all the other amino acids, can adopt neutral and ionic molecular forms. The prevailing one is related to the chemical environment and/or the pH of the solution. Three possible ionic forms of amino acids have been identified: cationic at acidic pH (amino group appears protonated), anionic at basic pH (carboxylic group appears deprotonated), and zwitterionic at neutral pH (amino group is protonated and carboxylic group is deprotonated).

However, due to its imidazole side chain, which can also be ionized, five ionic forms in total exist for histidine, which are shown in Figure 1. Each form may be distinguished by characteristic vibrational bands, associated with the main functional groups present. The H_4His^{2+} ionic form is identified by the COOH group giving a characteristic carboxylic band around 1740 cm^{-1}. All the other ionic forms bear a carboxylate group (COO^-) which is identified by the asymmetric and symmetric carboxylate stretches $\nu(COO^-)$ around 1620 and 1400 cm^{-1}, respectively. In addition to these easily detectable differences, the molecule has specific, charged or not, groups expected to yield characteristic vibrations (see Table 1). Starting with the first ionic form, each of the following ones will be identified by a characteristic feature change from the immediately previous ionic form. H_3His^{+} is identified by the presence of the carboxylate group and the ring being positively charged, H_2His^0 by neutral ring features, $HHis^-$ by the NH_2 group in place of the NH_3^+, and, finally, His^{2-} by the ring being negatively charged.[15]

Although each form can theoretically be identified by particular vibrational modes, the great number of absorption bands, the possible shifts due to surface interaction, and the modulation of intensities originating from surface selection rules make identification of the exact adsorbed form quite difficult. Our discussion will thus also rely on the histidine and imidazole ATR spectra as well as on the computed IR spectrum of the most abundant ionic form of adsorbed histidine.

3.2. IR-ATR Spectra of (*S*)-Histidine and Imidazole. The IR spectra, recorded in ATR mode on a germanium crystal, are reported in Figure 2. In the upper spectrum, IR characteristic bands of the imidazole ring modes can be identified following literature data.[29,30]

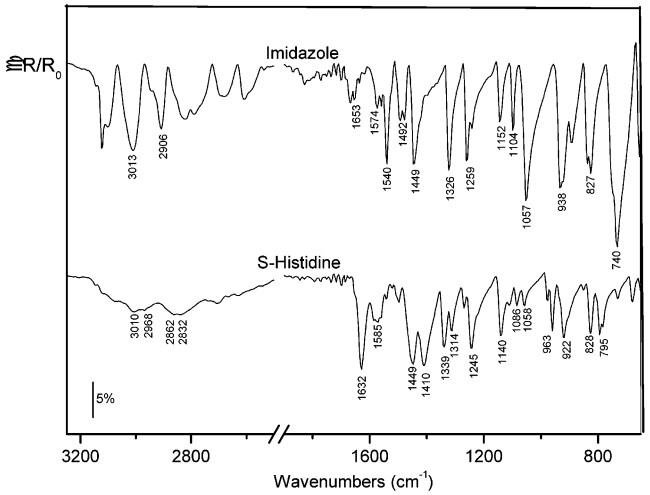

Figure 2. ATR-IR spectra of imidazole and (*S*)-histidine powder.

The bands present in the lower spectrum, that of histidine, were also identified following previous works.[18,31] All experimental data and the assignments are reported in the first two columns of Table 2

3.3. Adsorption of (*S*)-Histidine on Cu(110). *3.3.1. Nature of the Adsorbed Species*. Figure 3 shows the development of the RAIRS spectra with increasing exposure of (*S*)-histidine onto the Cu(110) surface at 300 K. Experimental infrared frequencies and band assignments are given in Table 2.[18] By comparing this set of data with those given in the literature for the various forms of histidine, one may now discuss which one is the most likely adsorbed on Cu(110) under our experimental conditions, knowing that small shifts can be observed due to interaction with the substrate.

The absence of the ν(C═O) stretching vibration around 1740 cm^{-1}, and the appearance of vibrations attributable to the COO^- functionality, excludes the possibility of H_4His^{2+} species adsorbed on Cu(110). Although distinction between NH_2 and NH_3^+ is rather difficult on the basis of IR data, the appearance of an intense band at 1580 cm^{-1}, readily ascribed to the $\delta(NH_2)$ scissors, supports the idea of the existence of a NH_2 group

TABLE 2: Infrared Assignments for Imidazole (ATR), (*S*)-Histidine (ATR), (*S*)-Histidine Adsorbed on Cu(110), and (*S*)-Histidine Adsorbed on the Top of a Preadsorbed Oxygen Layer on Cu(110)

		(*S*)-histidine− Cu(110)		(*S*)-histidine− O_2− Cu(110)			
imidazole (ATR)	(*S*)-histidine (ATR)	low coverage	high coverage	O_2-p(2×1)	O_2-p(6×2)	assignment	ref
3013	3010	3005	3013		3006	ring str	29
	2968		2954			CH_2 as str	
2906		2900	2905	2907	2902	ring str	
	2862		2874	2881		CH_2 s str	
	2832	2841	2842	2833	2833	CH str	
1670/1653		1650	1653		1652	(CC str + CNH def) ring	29, 30
	1632	1635	1636	1616	1635	COO^- as str	5−7
	1585	1577	1580	1589		NH_2 sciss	5, 6
1574	1571		1568	1574	1565	CC str ring	29
1558/1540	1557	1559/1540	1557/1544	1543	1544	(HNC def +	29, 30
1492		1507	1509	1523/1507	1522	HCC def) ring	
1476						ring str	29
1449	1449	1458/1442	1457/1442		1440	CH_2 sciss	5
	1410	1409	1414/1401	1422/1400	1401	COO^- s str	5−7
1326	1339			1340	1359	ring CH bend	29
	1314		1313	1310	1301	CH_2 wag/CH bend	5, 6
1259	1270	1294	1291			breath ring ip	29
1242	1245			1240/1210	1232	breath ring ip	29
1152	1140	1156	1154	1170	1191	(CN str + NH bend) ring	29, 30
1104	1111				1117	(CN str + CNC def) ring	30
	1086	1082	1082	1102	1103	NH_2 wag +	
1057	1058	1035	1024			CN str	5, 29
			1003	1004	1002	CH wag	
	979		988		968	ring def	5, 30
	963	952	974		950	CH_2 rock	5
938	922			914	927	ring bend	29
899		905/884	900/885	894		CH_2 wag ring	29, 30
838/827	828						
	795						
	784					COO^- sciss	6
740						ring torsion	30

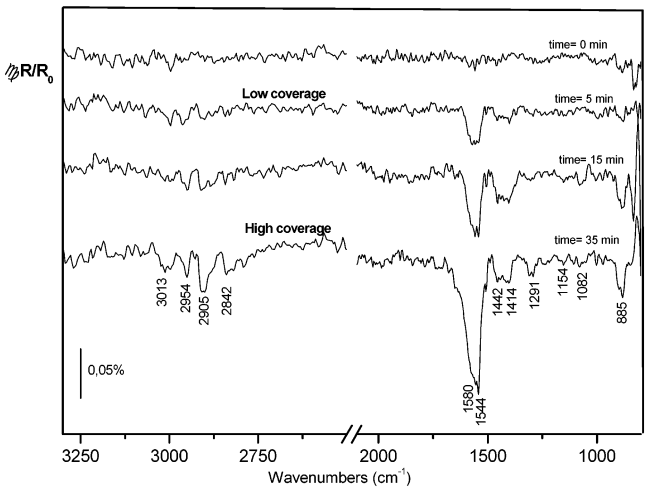

Figure 3. RAIRS spectra of (*S*)-histidine−Cu(110) at 300 K.

as a part of the adsorbed molecule. This result is in agreement with adsorption studies of other amino acids on Cu(110).[5,6] Therefore, H_3His^+ and H_2His^0 species will not be considered any more as possible adsorbed ionic forms. Finally, there are only two ionic forms still possible, $HHis^-$ and His^{2-}, identified by a neutral and a negatively charged imidazole ring, respectively. His^{2-} species only appear at very drastic conditions of pD > 12.2;[18] we hence propose that the $HHis^-$ ionic form is the one adsorbed on Cu(110). The presence of an N−H imidazole band at 1154 cm^{-1}, weak but still detectable, ascribed to the remaining NH group in the neutral ring, confirms this hypothesis. The existence of a mixture of different species adsorbed on the surface, some giving hardly detectable infrared signals, cannot be excluded, but the analysis indicates that the main adsorbed species is $HHis^-$.

The RAIRS data allow the kinetics of adsorption of the $HHis^-$ form of histidine on Cu(110) to be monitored. Figure 3 indicates that the coverage increases and reaches saturation after 30−40 min depending on the pressure inside the chamber ($\sim 2 \times 10^{-8}$ mbar).

The Auger spectra recorded after gas evacuation showed new features: carbon, nitrogen, and oxygen and a decrease in the copper peak (see Table 3), as expected after adsorption of the (*S*)-histidine molecule on the surface.

3.3.2. Orientation of the Adsorbed Species. The orientation of (*S*)-histidine on Cu(110), at saturation, will now be analyzed by applying the surface selection rule for RAIRS: *Only vibrational modes having a nonzero component of the dipole moment change normal to the surface will be observed.* This will be the basis for analyzing the vibrational bands associated with each functional group in the molecule (i.e., COO^-, NH_2, imidazole ring, CH_2, and CH groups).

Figure 4 shows the most relevant vibrations of the ring, and the local dipole moments associated with them, deduced from the MMFF calculations, making the following discussion easier.

Table 2 gives the assignments of the IR signals of the (*S*)-histidine adsorbed on Cu(110) at low and high coverage, in comparison with those from the ATR spectra of the molecule itself and of the imidazole ring. This enables a clear identification of the infrared bands ascribed to the ring, and those specific to the histidine molecule such as for COO^-, NH_2, CH_2, and aliphatic CH.

Starting the analysis with the COO^- group, the two expected vibrational modes are the asymmetric $\nu_{as}(COO^-)$ stretch and the symmetric $\nu_s(COO^-)$ stretch, whose intensities are strong

TABLE 3: Auger Signal Ratios

	Cu−hist	Cu−O-p(2×1)	Cu−O-p(2×1)−hist	Cu−O-p(6×2)	Cu−O-p(6×2)−hist
O_{503eV}/Cu_{60eV}	0.05	0.09	0.08	0.18	0.17
C_{272eV}/Cu_{60eV}	0.08	0.03	0.04	0.02	0.04
N_{398eV}/Cu_{60eV}	0.02	0.01	0.03	0.02	0.04

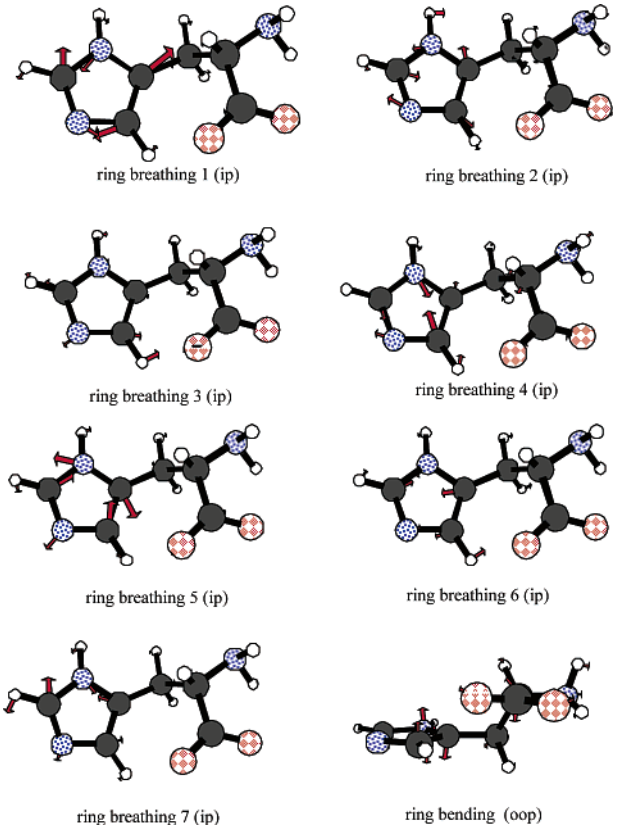

Figure 4. Principal vibrations associated with the (*S*)-histidine molecule (local dipole moments).

in the infrared spectra of the (*S*)-histidine powder and absent in the imidazole spectrum. Since in the RAIRS spectra only the $\nu_s(COO^-)$ stretch at ca. 1410 cm^{-1} is observed, the two carboxylate oxygen atoms must be placed equidistant from the copper surface; thus, the $\nu_{as}(COO^-)$ stretch will be dipole inactive. The plane of the carboxylate group with respect to the surface is probably tilted from the normal to the surface to explain the medium to weak intensity of the $\nu_s(COO^-)$ band.

Regarding the NH_2 group, the inherently strong $\delta(NH_2)$ scissors deformation at 1580 cm^{-1} and the associated wagging mode $w(NH_2)$ at 1082 cm^{-1}, normally weak, can be seen in the RAIRS spectra. This attribution is confirmed by the presence of these bands in the ATR histidine spectrum and their absence in the imidazole one (Figure 2). We deduce that the NH_2 group is orientated with its axial plane almost normal to the surface and the two hydrogen atoms equidistant to the surface, allowing the $w(NH_2)$ mode to be dipole active. A nearly perpendicular position of the NH_2 plane is in agreement with a strong intensity from the $\delta(NH_2)$ mode, at 1580 cm^{-1}; this signal may include a contribution from the in-plane (ip) ring breathing mode.

The weakness of the IR absorption at ca. 1035 cm^{-1}, the ν-(CN) region, indicates that the CN bond is almost parallel to the surface. Moreover, we think that the related NH_2 group will be held close to the surface, this geometry facilitating the interaction of the amino group with the copper atoms.[32,33]

The 3100−2800 cm^{-1} infrared region shows the absence of any intense feature for the CH and CH_2 stretching. Table 2 shows the assignment of asymmetric and symmetric CH_2 stretch

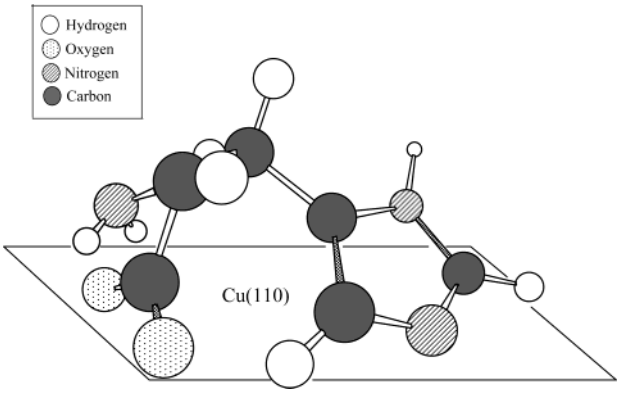

Figure 5. Orientation adopted by (*S*)-histidine on Cu(110).

modes at 2954 and 2874 cm^{-1} respectively, and the CH stretch mode at 2841 cm^{-1}. The weaker intensity of these bands in Figure 3, compared to those in Figure 2 (lower spectrum), suggests that the CH_2 and CH groups are tilted with respect to the metal surface. This orientation can be corroborated by the observance of signals at ca. 1444, 1291, and 952 cm^{-1} (very weak) usually ascribed to other CH_2 modes: CH_2 scissors, CH_2 wag, and CH_2 rock, respectively. Also detected in this geometry are the CH bending and CH wagging modes of the CH_2 group at 1313 and 1003 cm^{-1}, respectively.

As for the imidazole ring, the assignment of individual vibrational modes is especially difficult and complex due to numerous coupling modes within the cycle and between the cycle and adjacent groups (see Figure 4). The main feature in the RAIRS spectra is observed between 1577 and 1540 cm^{-1}, it is obviously due to the overlapping of the NH_2 scissors mode and the ip vibrational modes of the imidazole ring. This suggests that the ring tends to adopt a position perpendicular to the metal surface, possibly slightly tilted from the [110] direction, in agreement with the weak infrared absorption in the ring out-of-plane (oop) deformation spectral region (1000−920 cm^{-1}). Finally, the strong intensity of the ip bands, compared to the C−C, C−N, and N−H stretching bands, as well as the weakness of the C−H vibrational bands, is in good agreement with the proposed orientation of the molecule.

The $HHis^-$ form being the most abundant on the Cu(110) surface, with an upright, or almost upright, orientation of the imidazole ring on the surface, we propose that the molecule (*S*)-histidine is adsorbed on the Cu(110) surface as represented in Figure 5. The interaction between the ring and the copper surface via the deprotonated nitrogen of the imidazole ring will be demonstrated below.

3.4. Adsorption of (*S*)-Histidine after Preadsorption of Oxygen on Cu(110). *3.4.1. Preadsorbed Oxygen, p(2×1) Structure*. The development of RAIRS spectra of (*S*)-histidine after preadsorption of a low oxygen coverage (p(2×1) LEED pattern) is shown in Figure 6. These spectra show features rather similar to those of the RAIRS spectra of (*S*)-histidine on Cu-(110). The vibrational frequencies of (*S*)-histidine on Cu(110) and (*S*)-histidine on Cu(110)−O-p(2×1) are given in Table 2. The disappearance of a few bands and variations in the intensity and shape of some others suggest a slight reorientation of the molecule after preadsorption of oxygen on the surface.

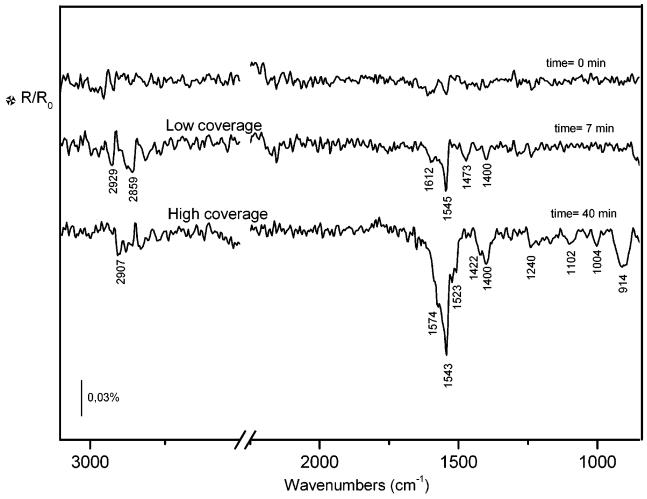

Figure 6. RAIRS spectra of (*S*)-histidine−oxygen-p(2×1)−Cu(110).

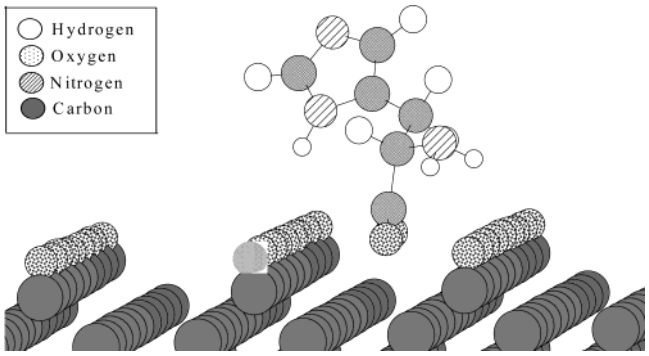

Figure 7. Orientation adopted by (*S*)-histidine−oxygen-p(2×1)−Cu-(110).

The main signals, which are the in-plane modes of the ring, become sharper and less intense in this case, which suggests a less upright orientation of the ring than in the previous case. The ring plane will remain close to the normal to the surface, as shown by the still intense in-plane modes in the RAIRS spectra. This change in the ring plane will force the reorientation of the aliphatic CH and the CH_2 groups. This is indeed confirmed by the decrease of the following bands: CH_2 scissors, CH_2 wag/CH bend, and ring deformation modes at 1457, 1313/1291, and 988 cm^{-1}, respectively, in the new spectra. Nevertheless, we do not exclude that these minor changes in the orientation of the molecule, indicated by the disappearance of some IR signals, are accompanied by a slight decrease in the coverage of histidine when oxygen is preadsorbed. The model proposed is shown in Figure 7.

After interaction of (*S*)-histidine and gas evacuation, an Auger spectrum was recorded, showing new features: the peak to peak Auger ratio O/Cu was hardly decreased, from 0.09 to 0.08; weak nitrogen and carbon peaks were detected, which corroborates a successful adsorption of the (*S*)-histidine on the preadsorbed oxygen-p(2×1) structure.

3.4.2. Preadsorbed Oxygen, c(6×2) Structure. Figure 8 shows RAIRS spectra of (*S*)-histidine after preadsorption of a higher dose of oxygen, (c(2×1) LEED pattern). In comparison with the previous spectra recorded on Cu(110)−O-p(2×1), neither disappearance of a feature nor a new feature in the spectra could be observed; this suggests that (i) oxygen does not block the adsorption of (*S*)-histidine and (ii) the interaction of the amino acid with the surface is not modified by the increase in the oxygen coverage.

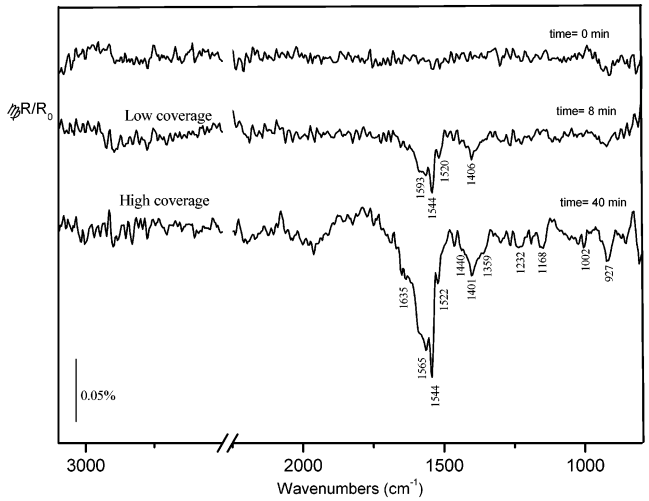

Figure 8. RAIRS spectra of (*S*)-histidine−oxygen-p(6×2)−Cu(110).

After interaction of (*S*)-histidine and gas evacuation, an Auger spectrum was recorded (see Table 3). Copper is strongly attenuated by the molecule. The peak to peak Auger ratio O/Cu hardly varies upon histidine adsorption due to the compensation of the attenuation of the oxygen, initially present, by the oxygen of the molecule. Finally, the appearance of two new features, carbon and nitrogen peaks, indicates that the adsorption of oxygen and (*S*)-histidine has been done successfully.

3.5. Modelization of the Adsorbed $HisCOO^-$. Since the experimental results clearly showed the carboxylate function and the amine group as a part of the adsorbed molecular species ($HHis^-$), we investigated the molecular conformation of the most probable ionic form of histidine in the adsorbed state. As the molecular ion $HHis^-$ has been experimentally evidenced on both the metallic and oxidized surfaces, we have only computed the $HHis^-$ adsorption on the Cu(110)−O-p(2×1) surface. We also checked the influence on the RAIRS spectrum of the heterocycle orientation, which seems to be affected when the copper surface is modified by oxygen. To describe the molecule approach onto the solid, the surface was reproduced by a truncated bulk structure and a point charge distribution with a Cu(110)−O-p(2 × 1) reconstruction geometry with about 1000 atoms in the ionic layer for the oxygen-modified surface. Molecular mechanics force field calculations well describe purely electrostatic interactions and molecular conformations for large molecules or proteins, and also give an excellent estimation of vibrational frequencies of organic molecules.[34] They will be applied to check the molecular geometry of histidine in the interaction with the surface.

First, the MMFF calculation led to an equilibrium geometry where the main interaction in the molecular adsorption process is governed by the attractive force between the negatively charged carboxylate group and the copper surface. On the Cu-(110)−O-p(2 × 1) surface, the carboxylate group of the $HHis^-$ entity is adsorbed over Lewis cationic sites located between Cu−O rows in the [001] direction (bidentate form), the COO^- plane being nearly parallel to this direction in agreement with the experimental results (Figure 9). Due to heterocycle and amine group interactions with the surface, a small tilt of the COO^- plane with respect to the [110] direction, as well as a small tilt between the carboxylate oxygen−oxygen axis and the (110) surface, is observed. The distance between the carboxylate oxygen atoms and the nearest positively charged copper ion is about 0.26 nm, in a good agreement with the expected values for carboxylic acid salts. For this computed adsorption equilibrium geometry, each of the carboxylate oxygen atoms is 0.33

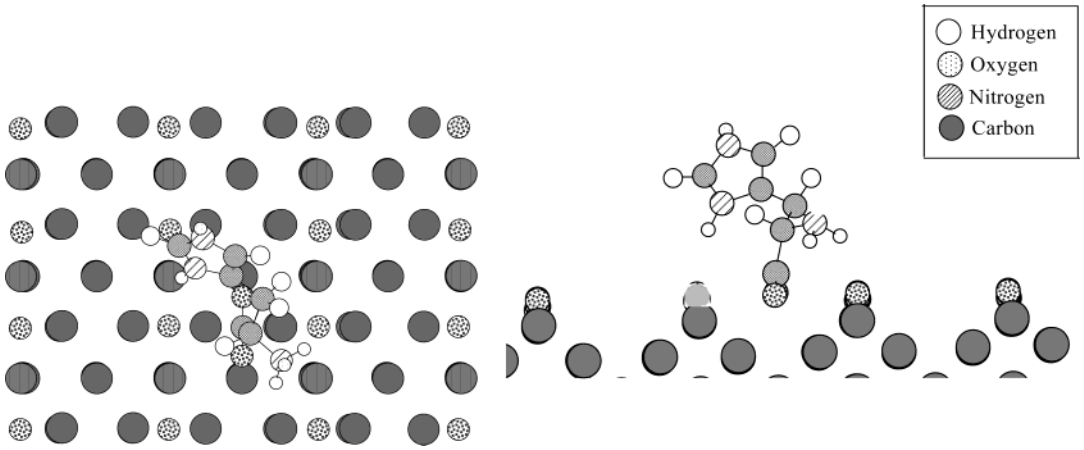

Figure 9. Orientation of $HHis^-$ on Cu(110)−O-(2×1) from MMFF calculation.

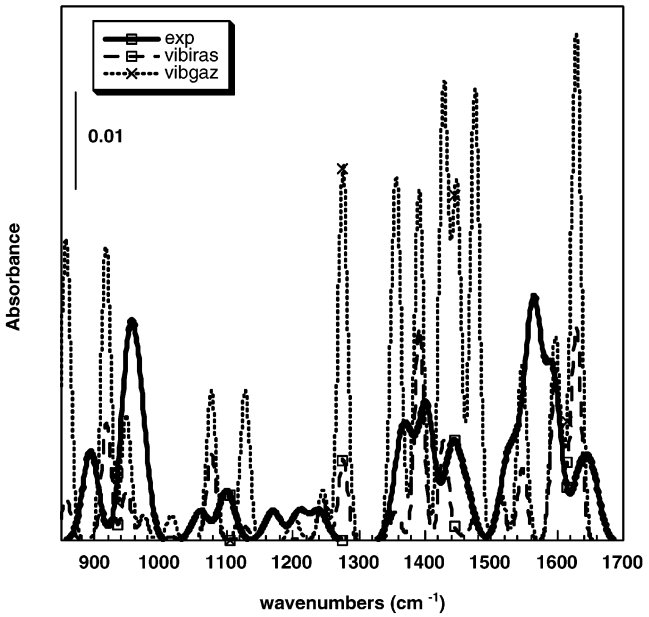

Figure 10. Comparison of experimental and computed spectra with and without surface selection rules.

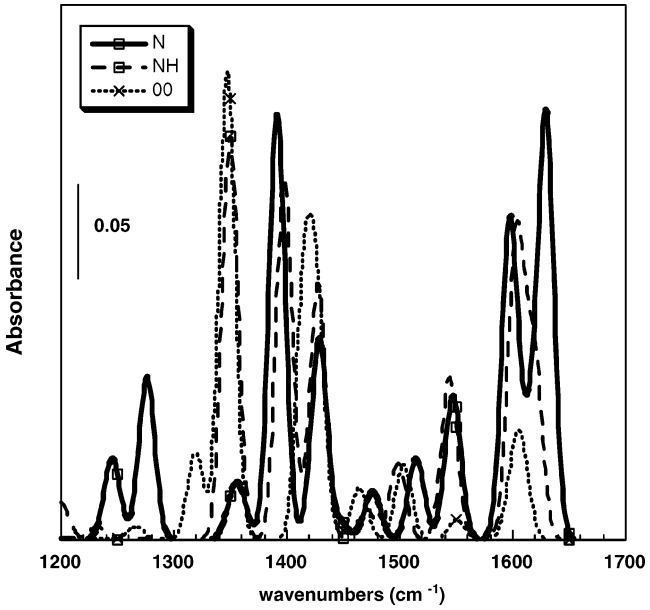

Figure 11. Ring orientation effect on the RAIRS spectra.

nm from the nearest anion of the Cu−O row. Concerning the amine group interaction, we found that the hydrogen atoms of the amine group point toward the O^{2-} anion and at a distance of 0.22 nm from this site, leading to a geometry where the NH_2 wagging mode (1102 cm^{-1}) should be active following RAIRS selection rules, and confirming our experimental observations.

The most informative part of the infrared spectra for the molecular orientation is the spectral range, where the heterocycle in-plane and out-of-plane vibrational modes appear. While in-plane cycle deformation modes should have strong intensities when the heterocycle is almost perpendicular to the surface, the out-of-plane deformation modes should have very weak intensities. Moreover, for $HHis^-$, 21 vibrational modes involving the heterocycle are expected, making uneasy the exact assessment of the cycle modes and orientation; the MMFF modelization and the computation of the vibrational spectrum will enable the conclusions drawn from experimental data to be checked. Figure 10 compares the spectrum reproduced by taking Gaussian peaks for all modes identified in the experimental spectrum and the computed spectrum, with and without surface selection rules. As IR absorption cross sections were not computed in the force field code, we took experimental intensities for each vibrational mode of histidine in the solid state (ATR spectrum). One can remark that the calculated vibrational frequencies are in good agreement with the experimental ones (by tenths of cm^{-1} or better) and that the main features of the vibrational spectrum between 800 and 1700 cm^{-1} are well reproduced. Figure 10 shows that RAIRS selection rules indeed strongly influence the spectral range between 1200 and 1700 cm^{-1} where the in-plane cycle deformation modes appear. As the cycle can interact with the surface by its NH (pyridine N or pyrrole N) chemical group, we then looked at different adsorbed geometries to clarify the effect of the cycle orientation on the vibrational spectra of the adsorbed molecule. We let the heterocycle plane change its orientation from the [110] direction by rotating the cycle around the C−C bond between the cycle and the CH_2 group in the adsorbed molecule. Note that the vibrational polarizability, e.g., the interaction of each dipole with its image, has not been considered in our calculation due to the complexity of the system. Figure 11 shows the computed spectra for three different orientations of the cycle and demonstrates the strong influence of the heterocycle orientation on the absorption peak intensities around 1500−1600 cm^{-1}. Other tilt angles (±20°, ±40°) were tested. The computed spectra were in strong disagreement with the experimental one and not worth being displayed. The first adsorbed geometry of Figure 11 ("OO") corresponds to the heterocycle parallel to the (110) plane, with no preference between NH and N interaction with the surface. The two other geometries approximately correspond

to the heterocycle plane tilted 70° from the (110) plane (Figure 9 configuration), one with the N atom ("N") and the other with the NH group ("NH") close to the surface. One interesting difference between the spectra of the N and NH adsorbed geometries concerns the absorption bands, located near 1280−1300 cm^{-1}, corresponding to in-plane ring deformation vibrational modes. From the MMFF calculation, one can see that the N geometry gives rise to an absorption band at ca. 1270 cm^{-1} whereas the NH geometry does not. This band was only observed when histidine was adsorbed on the metallic (110) surface; we thus conclude that the $HHis^-$ molecule is adsorbed with its cycle interacting by its pyridine N atom with a surface copper atom. On the contrary, when histidine is adsorbed onto the oxygen-modified surface, no band can be seen at 1300 cm^{-1}; the $HHis^-$ molecule is hence adsorbed with the NH heterocycle group interacting with surface sites (oxygen or copper). The same conclusion could be drawn from the change in the intensity of the signal at ca. 1350 cm^{-1} (ring CH bend). The latter, much weaker when the N geometry is adopted, confirms that the molecule is bound via its N atom on the metallic surface (see Table 2).

Other spectral evidences confirm these conclusions: a particularly interesting vibrational band is the one associated with the cycle NH deformation. Deformation modes of amines are indeed sensitive to the chemical bond with oxide surfaces.[35] On the metallic Cu(110) surface, this mode appears at 1154 cm^{-1}, while we can observe it at 1170 cm^{-1} when histidine is adsorbed on the oxygen-modified copper surface. As an increase in the $\delta(NH_{cycle})$ vibrational frequency was observed for the adsorbed $HHis^-$ molecule, one can conclude that this function is, in no case, involved in a dative bond with an electrophilic surface site cation, implying the nitrogen lone pair. Moreover, the increase of 16 cm^{-1} can be related to a hydrogen bonding known to lead to a blue shift of the bending NH mode;[36] this confirms our previous conclusion that, on the oxygen-modified surface, the imidazole cycle of the $HHis^-$ molecule interacts via its NH function pointed toward an oxygen anionic site.

To justify these conclusions about the cycle interactions with the metallic and oxygen-modified Cu(110) surface, simple arguments concerning steric hindrance as well as electronic structure calculation can be considered. From purely sterical effects, we expect that, on a metallic Cu(110) surface, the pyrrole-type nitrogen lone pair of the imidazole ring is more accessible to a copper surface site than is the lone pair of the pyridine nitrogen because of the presence of the hydrogen atom. On the contrary, on the oxygen-modified surface Cu(110)−O-p(2×1), as the oxygen anions are on the outer surface plane, cationic copper sites should be less accessible to the nitrogen lone pair and only a hydrogen bond with the NH function of the imidazole ring can be favored. From an electronic structure point of view, the hydrogen local positive charge of the NH group will favor the electrostatic interaction with a negatively charged oxygen anion in the Cu−O rows, leading to a hydrogen bond between the cycle NH function and the oxidized surface.

Conclusions

Adsorption of (*S*)-histidine on metallic Cu(110), and Cu(110) modified by adsorbed oxygen, has been studied. The surface chemistry and structure were controlled by Auger spectroscopy and LEED, respectively, while the adsorbed molecular entities were in-situ characterized by RAIRS. Force field calculation (MM2 and CHARMM potentials) were also used to confirm the molecular conformation of the adsorbed molecule. While five different ionic forms for histidine can be expected by protonation and/or deprotonation mechanisms in the adsorption process, we conclude that the molecule preferentially binds to the surface in its $HHis^-$ molecular form. Adsorption proceeds via the carboxylate group (COO^-), holding the two oxygen atoms nearly equidistant from the surface, and via the dehydrogenated nitrogen of the imidazole group, which adopts an upright position with respect to the copper surface. The amino group (NH_2) is maintained close to the surface, facilitating the interaction with the metallic surface.

Preadsorption of oxygen ($\theta \approx 0.3$) on the copper surface leads to a p(2×1) reconstruction and forces a readjustment of the molecular orientation. More interesting, an interaction of the NH group of the heterocycle with the Cu−O row of the Cu(110)−O-p(2×1) reconstruction now appears, compared to the previous analysis in the absence of oxygen. The molecule does not reorient with increasing oxygen coverage, p(2×2) ($\theta \approx 0.6$).

These results open new insights into the control of biomolecule−solid surface interactions.

References and Notes

(1) Ratner, B. D.; Hornell, T. A.; Shuttleworth, D.; Thomas, H. R. *J. Colloid Interface Sci.* **1981**, *83*, 630.
(2) Sundgren, J. E.; Bodo, P.; Lundstrom, I. *J. Colloid Interface Sci.* **1986**, *110*, 9.
(3) Storri, S; Santoni, T.; M. Minunni; Mascini, M. *Biosens. Bioelectron.* **1998**, *13*, (3−4), 347.
(4) Pradier, C.-M.; Salmain, M.; Zheng, L.; Jaouen, G. *Surf. Sci.* **2002**, *502−503*, 193−202.
(5) Barlow, S. M.; Kitching, K. J.; Haq, S.; Richardson, N. V. *Surf. Sci.* **1998**, *401*, 322.
(6) Williams, J.; Haq, S.; Raval, R. *Surf. Sci.* **1996**, *368*, 303.
(7) Mateo Marti, E.; Barlow, S. M.; Haq, S.; Raval, R. *Surf. Sci.* **2002**, *501*, 191.
(8) Brown, J. R. Structure of bovine serum albumin. *Fed. Proc.* **1975**, *34*, 591.
(9) Daeschel, M. A.; McGuire, J. *Biotechnol. Genet. Eng. Rev.* **1998**, *15*, 413.
(10) Rubio, C.; Costa, D.; Belon-Fontaine, M. N.; Relkin, P.; Pradier, C. M.; Marcus, P. *Colloids Surf., B* **2002**, *24*, 193−205.
(11) Servagent-Noinville, S.; Revault, M.; Quiquampoix, H.; Baron, M. H. *J. Colloid Interface Sci.* **2000**, *221*, 273.
(12) Pickup, M. E.; Dixon, J. S.; Lowe, J. R.; Wright, V. *J. Rheumatol.* **1980**, *7* (1), 71.
(13) Perrin, D. D.; Sharma, V. S. *J. Chem. Soc A* **1967**, 724.
(14) Williams, D. R. *J. Chem. Soc., Dalton Trans.* **1972**, 790.
(15) Martusevicius, S.; Niaura, G.; Talaikyte, Z.; Razumas, V. *Vib. Spectrosc.* **1996**, *10*, 271.
(16) Xue, G.; Dong, J.; Sun, Y. *Langmuir* **1994**, *10*, 1477.
(17) Walker, R. *Corrosion* **1975**, *31*, 97.
(18) Carlson, R. H.; Brown, T. L. *Inorg. Chem.* **1966**, *5*, 268.
(19) Freedman, J. H.; Davis, J. L.; Mims, W. B.; Peisach, J. *Inorg. Chim. Acta* **1983**, *79*, 218.
(20) Sundberg, R. J.; Martin, R. B. *Chem. Rev.* **1974**, *74*, 481.
(21) Pettit, D.; Swash, L. M. *J. Chem. Soc., Dalton Trans.* **1976**, 588.
(22) Perrin, D. D. *Nature* **1959**, *184*, 1868.
(23) Patel, V. K.; Bhattacharya, P. K. *Inorg. Chim. Acta* **1984**, *92*, 199.
(24) Leberman, R.; Rabin, B. R. *Trans. Faraday Soc.* **1959**, *55*, 1660.
(25) Allinger, N. L. *J. Am. Chem. Soc.* **1977**, *99*, 8127−8134.
(26) Brooks, B. R.; Bruccoleri, R. E.; Olafson, B. D.; States, D. J.; Swaminathan, S.; Karplus, M. *J. Comput. Chem.* **1983**, *4*, 187−217.
(27) Pappu, R. V.; Hart, R. K.; Ponder, J. W. *J. Phys. Chem. B* **1998**, *102*, 9725−9742.
(28) Gruzalski, G. R.; et al. *Surf. Sci.* **1985**, *151*, 430−446.
(29) Cordes, M.; Walter, J. L. *Spectrochim. Acta* 1967, *24A*, 237.
(30) Sadlej, J.; Jaworski, A.; Miaskiewicz, K. *J. Mol. Struct.* **1992**, *274*, 247.
(31) Garfinkel, D.; Edsall, J. T. *J. Am. Chem. Soc.* **1958**, *80*, 3807−3812.
(32) Bagus, P. S.; Hermann, K. *Phys. Rev. B* **1986**, *33*, 2987.
(33) Mocuta, D.; Ahner, J., Jr.; Yates, J. *J. Chem. Phys.* **1997**, *107* (15), 5968.
(34) A Pearlman, D.; Case, D. A.; Caldwell, J. W.; Ross, W. S.; Cheatham, T. E., III; DeBolt, S.; Ferguson, D.; Seibel, G.; Kollman, P. *Comput. Phys. Commun.* **1995**, *91*, 1−41.
(35) Fripiat, J. J.; Servais, A.; Léonard, A. *Bull. Soc. Chim. Fr.* **1962**, 635.
(36) Joesten, M. D.; Schaad, L. J. *H Bonding*; Marcel Dekker Inc.: New York, 1974.